Intended for CanJChem Dalhousie University Anniversary Special Edition (by invitation)

Hydrogen-bonded Networks in Oxygen-coordinated Monoamide Complexes of Zinc(II)

Leila Mokhtabad Amrei and René T. Boeré*

Graphical Abstract

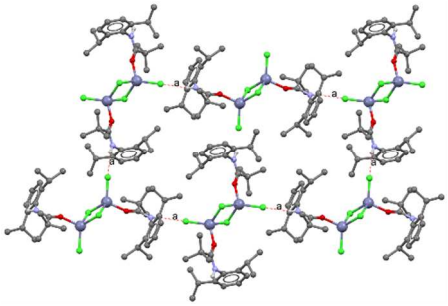

CJC does not use a separate TOC mini-abstract, but makes the full abstract available on the journal web page.

Keywords: synthesis; X-ray crystallography; hydrogen-bonding; graph sets; amide ligands

---

Leila Mokhtabad Amrei and René T. Boeré. Department of Chemistry and Biochemistry *and* the Canadian Centre for Research in Advanced Fluorine Technologies, University of Lethbridge, 4401 University Dr. W, Lethbridge, AB, Canada, T1K 3M4.

Corresponding author: René T. Boeré (e-mail: boere@uleth.ca). ORCID ID: orcid.org/0000-0003-1855-360X

This article is part of a Special Issue conceived to celebrate the 200th anniversary of Dalhousie University. The senior author is an alumnus and remembers the learning environment as stimulating and supportive.

Abstract: The preparation of the bulky secondary amide *N*-(2,6-diisopropylphenyl)-2,2-dimethylpropanamide and the determination of its crystal structure at 173(2) K are reported. The structure displays disorder of the ^{t}Bu methyl groups due to thermal motion and an infinite N–H····O=C hydrogen bonded chain described by a $C_1^1(4)$ graph set. Reaction of this amide with $ZnCl_2$ or $ZnBr_2$ in tetrahydrofuran (THF) results in dihalo-(tetrahydrofurano)-(*N*-(2,6-diisopropylphenyl)-2,2-dimethylpropanamido)-zinc(II) complexes (Cl, Br) for which the crystal structures have also been determined. These complexes, as well as a chloroform solvate of the dichloro-complex, contain N–H····X-Zn hydrogen bonded chains described by $C_1^1(6)$ graph sets. Evaporative crystallization results in the loss of both chloroform and THF to afford crystals determined to be *bis*(μ_2-chloro)-dichloro-*bis*(*N*-(2,6-diisopropylphenyl)-2,2-dimethylpropanamido)-dizinc(II) by single crystal X-ray diffraction. This dimeric complex shows a complex network of N–H····Cl-Zn hydrogen bonds describable by $C_1^1(6)$, $C_1^1(8)$ and $C_2^2(16)$ chains, small $R_4^4(28)$ molecular "squares" and larger $R_6^6(44)$ rings.

Résumé : La préparation de l'amide secondaire volumineux *N*-(2,6-diisopropylphényl)-2,2-diméthylpropanamide et la détermination de sa structure cristalline à 173(2) K sont rapportées. La structure présente le désordre des groupes méthyle du ^{t}Bu en raison du mouvement thermique et une chaîne linéaire N-H····O = C hydrogène infinie décrite par un ensemble de graphe $C_1^1(4)$. La réaction de cet amide avec $ZnCl_2$ ou $ZnBr_2$ dans le tétrahydrofurane (THF) conduit à des complexes dihalo-(tétrahydrofurano)-(*N*-(2,6-diisopropylphényl)-2,2-diméthylpropanamido)-zinc (II) (Cl, Br) pour lesquels les structures cristallines ont également été déterminées. Ces complexes, ainsi qu'un solvate chloroforme du dichloro-complexe, contiennent des chaînes N-H····X-Zn liées à l'hydrogène décrites par des ensembles de graphiques $C_1^1(6)$. La cristallisation par évaporation entraîne la perte de chloroforme et de THF pour donner des cristaux déterminés comme *bis*(μ_2-chloro)-dichloro-bis(*N*-(2,6-diisopropylphényl)-2,2-diméthylpropanamido)-dizinc(II) par diffraction des rayons X monocristallins. Ce complexe dimère présente un réseau complexe de liaisons hydrogène N-H····Cl-Zn descriptible par chaînes des $C_1^1(6)$, $C_1^1(8)$ et $C_2^2(16)$, petites "carrés" moléculaires de $R_4^4(28)$ et plus grands anneaux de $R_6^6(44)$.

Introduction

Amides **A** (Chart 1) are relatively less-common coordination ligands despite their high prevalence as components of natural and synthetic macromolecules (i.e. proteins and polymers).[1,2] Zinc is the second-most abundant d-block metal in mammals after iron and it plays crucial roles in many important biological processes.[3] These include structural and catalytic cofactors for enzymes, acting as neural signal transmitters or modulators, and in the regulation of gene expression and apoptosis.[4,5] Zinc is also a very important metal for polyamide coordination e.g. in ubiquitous zinc-proteins.[6,7] Recently, three aryl acetamide L_2ZnCl_2 complexes were reported with demonstrated antileishmanial and antiproliferative effects.[8] The polymeric chain [(*R*,*R*)-1,2-diacetamidocyclohexanedibromozinc(II)]$_n$ has been structurally characterized as a peptide model.[9] An asymmetric monoxo-tetraamine, a cyclic amide, has been utilized as an acceptor for glycine.[10]

Most third-period metals coordinate to amides *via* the carbonyl oxygen as donor and the nitrogen is by contrast a poor donor, in line with the canonical resonance structures that involve nitrogen free-electron pairs in partial π-bonding to the central carbon atom. Thus, as hard-base ligands, the coordinative preference is for hard-acid metals and zinc is particularly prevalent for oxygen-bound amide complexes. Most zinc-amide complexes are found to have the ML_2 stoichiometry, for which *bis*(acetamide-*κO*)diiodidozinc(II) is a typical example [11] and the number of zinc halide complexes with a single amide ligand are extremely limited.[12,13] Exceptions to this rule are almost always with chelating ligands that incorporate amide donors along with other strong donor sites, such as the substituted pyridylmethylamide complexes reported by Chaudhuri *et al*.[14]

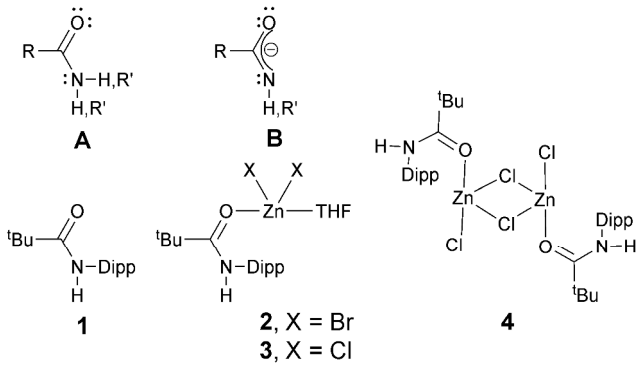

Chart 1. Line diagrams of the discussed structures

Deprotonated amidates **B**, mononegative and usually bidentate O,N donors, have increasing importance as supporting ligands in organometallic complexes and in catalysis, where the hybrid hard/medium-soft donor character is thought to offer important contrast to other heteroallylic ligand frameworks, such as the hugely important amidinates. Our work has focused on very bulky amides regarding a research program on low-coordinate phosphorus compounds as complex ligands. During this work, we developed the chemistry of the 2,6-diisopropylphenyl (Dipp) amide of several carboxylic acids including the pivalamide (i.e. ^{t}Bu) **1** (see Chart 1).

Using amide **1**, rare 1:1 metal-to-amide ratio complexes were prepared with zinc(II) chloride and zinc(II) bromide (Chart 1). To complete the coordination sphere of the metal (four coordinate, *pseudo*tetrahedral, as typical of this metal ion), THF from the synthesis reaction is strongly retained by the metal. For the chloro-complex, a second polymorph was obtained as a chloroform solvate. Slow evaporative crystallization of solutions of the chloro-complex also afforded $[ZnCl_2L]_2$ complexes which have lost the THF and which crystallize as a $(\mu_2Cl)_2$ doubly chloro-bridged structure. All these metal complexes display interesting and rare supramolecular hydrogen-bonding networks involving the amide NH donating to the coordinated halogens of a neighbouring molecule. Amidate complexes formed by deprotonation of **1** have recently been reported by others.[15-18]

Experimental

General methods

Solvents were reagent grade or better. Pyridine (Aldrich) was dried by standing over activated molecular sieves (4 Å). Trimethylacetyl chloride (Aldrich) was used as received and 2,6-diisopropylphenylanilene (Aldrich) was purified by reduced pressure distillation. Zinc bromide was dried by heating in vacuo at 300°C for 1 H.[19] $ZnCl_2(THF)_2$ was prepared by a literature procedure.[20] NMR spectra were recorded in $CDCl_3$ solution (^{1}H and ^{13}C) on a 300 MHz Bruker Avance II spectrometer and are referenced to the solvent residuals. Infrared data were collected at RT on a Bruker Alpha FTIR spectrometer (diamond ATR attachment). Elemental analyses were

obtained on a Vario Elementar micro-Cube analyzer. ESI mass spectra were measured on a Thermo Instruments ESI Mass Spectrometer as THF solutions.

Preparation of *N*-2,6-diisopropylphenylpivalamide or ^{t}Bu-amide 1

Trimethyl acetyl chloride (14.0 mL, 113 mmol) was carefully pipetted into a solution of 2,6-diisopropylaniline (20.0 g, 113 mmol) in 200 mL of dry pyridine (CAUTION: vigorous reaction, use cooling) followed by heating the mixture to reflux for 3 H. The solvent was removed, and the residues taken up in 200 mL CH_2Cl_2 and washed twice with 200 mL water. After drying and removal of solvent, the crude product was recrystallized from toluene to give colourless crystals. Yield: 24.6 g, 83%. MP: 254-255°C. ^{1}H NMR ($CDCl_3$): δ 1.20 (d, $^{3}J_{HH}$ = 6.9 Hz, 12H, CH(CH_3)$_2$), 1.36 (s, 9H, C(CH_3)$_3$), 3.01 (sept, $^{3}J_{HH}$ = 6.9 Hz, 2H, CH(CH$_3$)$_2$), 6.83 (br, 1H, N-*H*), 7.16 (d, $^{3}J_{HH}$ = 7.5 Hz, 2H, *m*-Dipp), 7.28 (t, $^{3}J_{HH}$ = 7.5 Hz, 1H, *p*-Dipp). ^{13}C NMR ($CDCl_3$): δ 23.7 (CH(*C*H$_3$)$_2$), 27.9 (C(*C*H$_3$)$_3$), 28.8 (*C*H(CH$_3$)$_2$), 39.4 (*C*(CH$_3$)$_3$), 123.5 (*m*-Dipp), 128.3 (*p*-Dipp), 131.6 (*ipso*-Dipp), 146.3 (*o*-Dipp), 177.4 (*C*O). IR (Diamond ATR) cm^{-1}: 3315 (s, N-H), 2960 (vs), 2868 (m), 1646 (vs, CO), 1501 (vs), 1469 (s), 1443 (m), 1361 (w), 1331 (w), 1257 (w),1209 (m), 1168 (m), 934 (s), 807 (m), 789 (s), 735 (vs), 655 (vs), 548 (s), 411(w). E.A. Calc. for $C_{17}H_{27}NO$: C, 78.11; H, 10.41; N, 5.36. Found: C, 78.06; H, 10.13; N, 5.33.

Preparation of dibromo-tetrahydrofurano-*N*-2,6-diisopropylphenylpivalamidezinc(II), 2.

Zinc dibromide (0.86 g, 3.8 mmol) was added into a solution of amide **1** (1.00 g, 3.83 mmol) in 30 mL of tetrahydrofuran, after which the mixture was stirred overnight to afford a clear solution. Solvent was removed by rotary evaporation and the crude product was then hot filtered and recrystallized from $CHCl_3$ to afford colorless crystals. Yield: 0.86 g, 40.0%. MP: 264-267°C. ^{1}H NMR ($CDCl_3$): δ 1.20 (d, $^{3}J_{HH}$ = 6.9 Hz, 12H, CH(CH_3)$_2$), 1.46 (s, 9H, C(CH_3), 1.76 (pent, $^{3}J_{HH}$ = 6.9 Hz, 4H, CH_2-THF), 2.95 (sept, $^{3}J_{HH}$ = 6.9 Hz, 2H, CH(CH$_3$)$_2$), 3.63 (pent, $^{3}J_{HH}$ = 6.9 Hz, 4H, OCH_2-THF), 7.19 (d, $^{3}J_{HH}$ = 7.5 Hz, 2H, *m*-Dipp), 7.32 (*t*, $^{3}J_{HH}$ = 7.5 Hz, 1H, *p*-Dipp), 7.38 (s, N*H*, 1H). ^{13}C NMR ($CDCl_3$): δ 23.75 (*C*H$_2$-THF), 25.34 (CH(*C*H$_3$)$_2$), 28.01 (C(*C*H$_3$), 28.91 (*C*H(CH$_3$)$_2$), 39.66 (*C*(CH$_3$)$_3$), 69.29 (*C*H$_2$O-THF), 123.73 (*m*-Dipp), 129.00 (*p*-Dipp), 130.70 (*ipso*-Dipp), 146.36 (*o*-Dipp), 180.63 (*C*O). IR (Diamond ATR) cm^{-1}: 3313 (s, N-H), 2962 (vs), 2932 (w), 2869 (w), 1599 (vs, CO), 1580 (s, CO), 1518 (vs), 1465

(w), 1442 (w), 1383 (m), 1214 (m), 1026 (s), 955 (m), 872 (s), 807 (s), 796 (m), 744 (s), 650 (m), 547 (w). MS (*m/z*): 665.26 (L_2ZnBr^+, 1.1%); 476.11 ($THFLZnBrTHF^+$, 6.5); 404.05 ($LZnBr^+$, 6.5); 262.22 (LH^+, 100); 220.17 (L – $3(CH_3)^+$, 12.5). Crystals kept at RT slowly lose THF (as confirmed by NMR integration) and a fitting EA has not been obtained.

Preparation of dicloro-tetrahydrofurano-*N*-2,6-diisopropylphenylpivalamidezinc(II), 3

$ZnCl_2(THF)_2$ (0.54 g, 1.92 mmol) was added into a solution of ligand (L= ^{t}BuCONDipp) **1** (0.50 g, 1.92 mmol) in 30 mL of tetrahydrofuran, then the mixture was stirred overnight. Solvent was removed by rotovap and the crude product was hot filtered and recrystallized from chloroform to give colorless crystals. Yield: 0.48 g, 41.0%. ^{1}H NMR ($CDCl_3$): δ 1.19 (d, $^3J_{HH}$ = 6.9 Hz, 12H, $CH(CH_3)_2$), 1.42 (s, 9H, $C(CH_3)$), 1.75 (pent, $^3J_{HH}$ = 6.9 Hz, 4H, CH_2-THF), 2.94 (sept, 2H, $CH(CH_3)_2$), 3.64 (pent, $^3J_{HH}$ = 6.9 Hz, 4H, OCH_2-THF), 7.17 (d, $^3J_{HH}$ = 7.5 Hz, (2H, *m*-Dipp), 7.30 (t, $^3J_{HH}$ = 7.5 Hz, 1H, *p*-Dipp), 7.34 (s, 1H, N-*H*). IR (Diamond ATR) cm^{-1}: 3313 (s, N-H), 2962 (vs), 2870 (w), 1646 (w), 1601 (vs, CO), 1581 (s, CO), 1521 (vs), 1467 (w), 1444 (w), 1362 (w), 1259 (s), 1026 (vs), 956 (m), 875 (m), 796 (vs), 744 (s), 662 (m), 548 (w). Crystals kept at RT slowly lose THF (as confirmed by NMR integration) and a fitting EA has not been obtained.

X-ray Crystallography

Crystals of **1** were grown by cooling hot solutions in toluene. Crystals of **2** and **3** grew from $CHCl_3$ as THF solvates.. Crystals of **4** grew from slow evaporation of an NMR sample of **3** out of $CDCl_3$ solution. Crystals were selected under a microscope to be optically free of obvious twins or multiples, then mounted on fine glass capillaries in Paratone™ oil. The crystals were cooled to 173(2) K in the cold N_2 stream of the diffractometer Kryoflex device and hemispheres of data collected on a Bruker Smart ApexII diffractometer [21] using Mo Kα radiation with SAINT-Plus,[21] which was also used to determine the unit cells, correct and integrate the data and determine the space groups. Structures were solved using direct methods in SHELXS [22] or intrinsic phasing in SHELXT.[23] Data refinement was undertaken with SHELXL-2014 using Olex2.[24,25]

141

Table 1. Crystal and Refinement Parameters for Structures **1** – **4**

Param.	**1**	**2**	**3**	**3a**	**4**
Formula	$C_{17}H_{27}NO$	$C_{21}H_{35}Br_2NO_2Zn$	$C_{21}H_{35}Cl_2NO_2Zn$	$C_{22}H_{36}Cl_5NO_2Zn$	$C_{17}H_{27}Cl_2NOZn$
FW	261.39	558.69	469.77	589.14	397.66
T/K	173.15	173.15	173.15	173.15	173.15
Crystal system			Monoclinic		
Space group	$P2_1/c$	Cc	Cc	$P2_1/c$	$P2_1/n$
a/Å	10.134(5)	14.1856(8)	13.9291(16)	20.302(8)	8.6018(14)
b/Å	18.359(9)	10.8746(6)	10.7019(13)	8.929(3)	14.238(2)
c/Å	9.873(5)	16.5621(9)	16.583(2)	17.068(5)	16.507(3)
β/°	116.471(5)	106.4390(10)	106.417(2)	114.751(3)	92.272(2)
V/Å^3	1644.3(13)	2450.5(2)	2371.2(5)	2809.9(16)	2020.1(6)
Z	4	4	4	Z	4
ρ_{calc} g·cm^{-3}	1.056	1.514	1.316	1.393	1.308
μ/mm^{-1}	0.064	4.278	1.276	1.368	1.481
F(000)	576	1136	992.0	1224.0	832.0
Crystal size/mm^3	0.305×0.143×0.1 14	0.323×0.153×0.1 33	0.174×0.104×0.0 65	0.378×0.285×0. 21	0.361×0.357×0.2 24
Radiation			MoK_α (λ = 0.71073 Å)		
2Θ range/°	4.438, 54.92	4.796, 54.742	4.876, 54.938	4.418, 52.988	3.778, 55.106
Index ranges, *h*	−13, 13	−18, 18	−18, 17	−25, 25	−11, 11
k	−23, 23	−13, 14	−13, 13	−11, 11	−18, 18
l	−12, 12	−21, 21	−21, 21	−21, 21	−21, 21
Tot. refl.	23416	16971	16978	35494	25622
Indep. refl.	3757	5471	5367	5739	4644
R_{int}	0.0392	0.0170	0.0818	0.0504	0.0670
R_{sigma}	0.0279	0.0332	0.1101	0.0345	0.0522
Data/restr/param	3757/60/225	5471/3/255	5367/3/255	5739/288/309	4644/0/209
GOF on F^2	1.030	1.020	0.964	1.128	1.020
Flack x		0.008(7)	0.048(19)		
Final R [I≥2σ(I)]	R_1 = 0.0477 wR_2 = 0.1176	R_1 = 0.0184 wR_2 = 0.0413	R_1 = 0.0517 wR_2 = 0.0784	R_1 = 0.0765 wR_2 = 0.2087	R_1 = 0.0471 wR_2 = 0.0854
Final R [all data]	R_1 = 0.0735 wR_2 = 0.1382	R_1 = 0.0201 wR_2 = 0.0417	R_1 = 0.1002 wR_2 = 0.0913	R_1 = 0.0893 wR_2 = 0.2181	R_1 = 0.1000 wR_2 = 0.1089
Larg. diff. peak/hole /e·Å^{-3}	0.26/−0.17	0.36/−0.39	0.34/−0.38	2.14/−1.09	0.62/−0.79

During the refinement of **1**, the ^{t}Bu group was modelled as a two-component rotational disorder; the central C of the ^{t}Bu group and the amide oxygen were included in the disordered components but the amide C and N atoms do not appear to be involved in the disorder. The disorder occupancies refined to 0.75/0.25 with strong restraints required to adequately refine the minor component atoms. The disorder appears as a dominant preferred orientation along with smaller components due to thermal excitation to other sites. Distance

restraints were employed for the N-H refinement (0.88 ± 0.10 Å) of **2**. In final cycles of refinement of **3a** a large residual peak with 2.1 e·Å^3 was left at 1.25 Å C17, which does not fit well for a ^{t}Bu rotational disorder; it looks more like a 'ghosting' behaviour from a possible minor twin component or other data errors. In view of the high quality of the non-solvated parent structure **3** the decision was taken not to pursue this matter further.

A two-part disorder model was developed for the ring twist in the coordinated THF molecule (atoms C20 and C21 only) with equal occupancy (see Figure S5b). In final refinement of the structure of **4**, rather large displacement ellipsoids were found for the ^{i}Pr methyl carbons C10 and C12 and ^{t}Bu carbons C15 and C16. A two-part disorder model for both features was developed which refined to 83:17 and 54:46 fractional occupancies, but the conventional *R* factor dropped by only 0.13% and some bond distances became unrealistic despite restraints. The decision was therefore taken to stick with an ordered model and accept the rather large displacement ellipsoids for the affected atoms. Post-refinement data analysis and graphics were undertaken using Mercury CSD release 3.9.[26] Crystal and refinement data are compiled in Table 1, significant intermolecular dimensions in Table 2 and hydrogen-bonding parameters in Table 3.

Results and Discussion

Complexes of **1** with zinc(II) chloride and zinc(II) bromide were prepared using tetrahydrofuran (THF) as solvent (Scheme 1), and despite recrystallization from chloroform, show a strong tendency to retain coordinated THF. The dibromo complex **2** is formed directly from recrystallization in $CHCl_3$, whereas the dichloro can be prepared either as the analogous **3** or as a $CHCl_3$ solvate **3a**, depending on recrystallization conditions. Moreover, only one equivalent of amide ligand is found to coordinate to the metal as could be shown by integration of the NMR signals (1:1 ratio of the amide and THF). The complexes are fully characterized by spectroscopy and single-crystal X-ray diffraction analysis (see Experimental for details). The ν(N–H) stretch of 3313 cm^{-1} in **1** remains unchanged in **2** and **3a** despite the change from oxygen to halide as hydrogen-bond acceptors. However, the ν(C=O) band, at 1646 cm^{-1} in **1**, undergoes coordination shifts as well as splitting into stronger

asymmetrical and weaker symmetrical modes at 1599 / 1580 cm^{-1} in **2** and 1601 / 1581 cm^{-1} in **3**. Such reduction in stretching frequencies by 45 – 47 cm^{-1} is diagnostic for oxygen coordinated amides.[8,14]

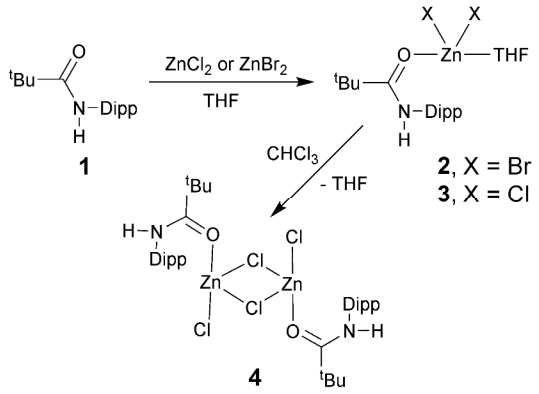

Scheme 1. Synthesis of the complexes

The neutral amide ligand structure **1** (Figure 1) displays typical ^{t}Bu group positional disorder due to thermal motion despite the 173 K data collection. This was modelled with two complete ^{t}Bu groups and the associated carbonyl oxygen atoms, in 75:25 ratio (see Figure S1 in the Supporting Information). Interestingly, while our work was in progress, another structure of the same polymorph as **1** was reported from a dataset collected at an unusually low 90 K as CSD refcode (Cambridge Crystallographic Database [27] release 5.38 updated to May 2017: ICEXEW), in which the thermal motion is fully supressed.[15] The methyl positions in ICEXEW correspond to the major conformer in our disorder model. These results emphasize the importance of very low temperature data collection for organic crystal structures that are susceptible to displacement disorders. All the bond distances in **1** are within 1% of those in the lower temperature structure, as are most angles except two associated with the O1, likely due to the disorder model used for **1**. Perhaps surprisingly, for all parameters except those involving disordered atoms, the standard uncertainties (s.u.) for **1** are lower, usually by about half, than reported for ICEXEW.[15] Additionally, the N–H bond length in the 100 K structure was not refined although it is hydrogen bonded (see below). For these reasons, structural analysis and comparison in this work will be based on our own crystal structure of **1**.

193 **Table 2**. Selected bond distances (Å) and angles (°) in the X-ray structures of **1** - **4**

Parameter	**1**	**2**	**3**	**3a**	**4**	**Mean** [a]
Zn–X1	—	2.3418(4)	2.204(2)	2.2236(15)	2.3250(11)	2.25(5) *
Zn–Cl1’	—	—	—	—	2.2996(11)	
Zn–X2	—	2.3187(4)	2.182(2)	2.1866(16)	2.1827(11)	2.1836(17) *
Zn–Zn’	—	—	—	—	3.1584(9)	
Zn–O1	—	1.9723(18)	1.974(4)	1.986(4)	1.937(2)	1.967(18) †
Zn–O2	—	2.032(2)	2.030(5)	2.022(4)	—	2.028(5) ‡
O1–C13	1.224(7)	1.243(3)	1.248(6)	1.247(6)	1.253(4)	1.248(4) †
N1–C1	1.4383(18)	1.442(3)	1.451(7)	1.449(7)	1.445(5)	1.447(3) †
N1–H1	0.891(16)	0.77(2)	0.86(3)	0.98(9)	0.84(4)	0.86(6)
N1–C13	1.3409(17)	1.328(3)	1.323(7)	1.323(6)	1.321(4)	1.324(3) †
C1–C2	1.4007(19)	1.397(4)	1.385(8)	1.402(7)	1.402(6)	1.397(7) †
C1–C6	1.3991(19)	1.402(4)	1.400(9)	1.389(7)	1.389(5)	1.394(8) †
C13–C14	1.540(5)	1.528(4)	1.511(8)	1.511(7)	1.516(5)	1.517(7) †
X2–Zn–X1	—	122.86(2)	122.44(10)	121.38(6)	115.18(5)	122.2(6) ‡
Cl1–Zn–Cl1’	—	—	—	—	93.85(4)	—
Cl2–Zn–Cl1’	—	—	—	—	119.84(5)	—
O1–Zn–X1	—	112.26(6)	113.27(15)	114.87(12)	100.91(8)	113.5(11) ‡
O1–Zn–X2	—	111.43(6)	111.15(15)	108.32(12)	112.60(9)	110.3(14) ‡
O1–Zn–O2	—	93.55(8)	92.51(16)	93.49(15)	—	93.2(5) ‡
O1–Zn–Cl1’	—	—	—	—	111.55(9)	—
O2–Zn–X1	—	106.22(6)	106.62(16)	104.21(12)	—	105.7(10) ‡
O2–Zn–X2	—	105.93(6)	106.05(16)	110.80(14)	—	108(2) ‡
Zn1–Cl1Zn	—	—	—	—	86.15(4)	—
C13–O1–Zn	—	145.80(19)	145.1(4)	145.8(3)	145.7(2)	145.6(3) †
C13–N1–C1	123.28(11)	122.5(2)	122.6(5)	122.1(4)	124.4(3)	122.9(9) †
C2–C1–N1	119.16(12)	118.4(2)	118.0(6)	117.7(4)	118.0(3)	118.0(3) †
C6–C1–N1	118.47(11)	118.5(2)	117.8(6)	119.0(4)	118.8(4)	118.5(5) †
C6–C1–C2	122.33(12)	123.1(3)	124.2(6)	123.3(4)	123.1(4)	123.5(4) †
N1–C13–C14	116.2(2)	118.8(2)	118.8(5)	119.1(4)	118.0(3)	118.7(4) †
O1–C13–C14	123.5(4)	122.4(2)	121.9(6)	121.5(4)	123.9(3)	122.5(9) †
O1–C13–N1	120.0(4)	118.8(2)	119.3(5)	119.2(4)	118.0(3)	118.8(5) †

194 [a] Mean values are taken over: * **3**, **3a**, **4**; † **2**, **3**, **3a**, **4**; ‡ **2**, **3**, **3a**. S.u. of the mean are standard deviations.

195

196 In this structure, **1** forms an infinite N–H···O=C hydrogen bonded chain described by a $C_1^1(4)$ graph set,[28]
197 strictly parallel to the crystallographic *c* axis (see Figure 1 and Table 3). The amide molecules are arranged in
198 alternating “up” / “down” fashion along the crystallographic *c* glide plane. In a space-filling view (Figure S2 in
199 the Supporting Information) this results in spherical ^{t}Bu cavities that fit between Dipp aryl rings in repeated
200 ‘catchers-glove/ball’ arrangements. The cavities thus created are evidently large enough to allow for ^{t}Bu group
201 rotation within the lattice at elevated temperatures.

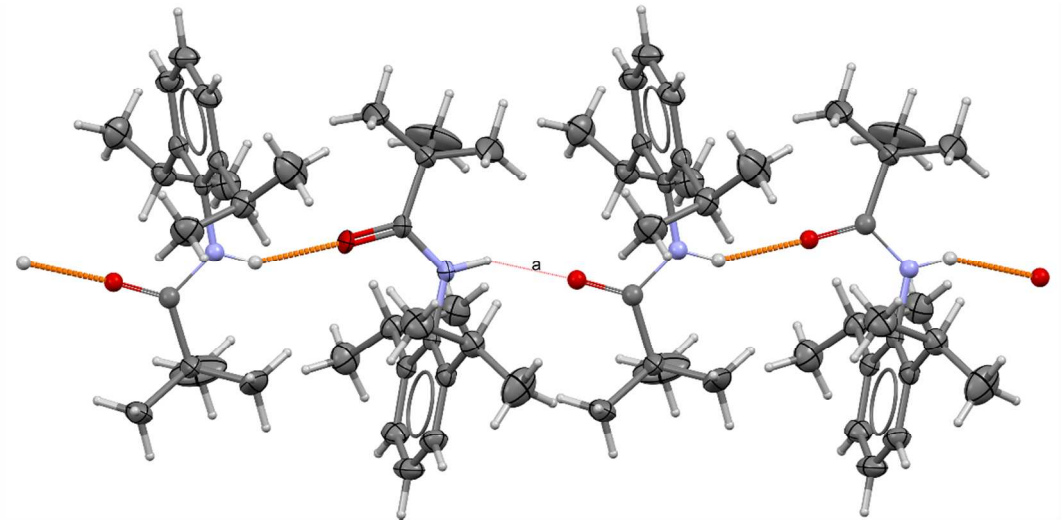

Figure 1. The hydrogen-bonding chain in the crystal lattice of **1** along the crystallographic *c* axis with alternating 'up' and 'down' amides. Grey = C, white = H, red = O, blue = N. The $C_1^1(4)$ graph set is identified at 'a'.

The complex with zinc(II) bromide, **2**, consists of the amide in an extremely similar conformation to that found in the structure of **1**, but now with the $ZnBr_2$·THF moiety attached to O1, with a very large C13-O1-Zn angle [145.80(19)°] but a very sharp O1-Zn-O2 angle [93.55(8)°] which allows the coordinated THF molecule to be positioned above the Dipp aryl ring (Figure 2). This results in co-planarity of atoms C4, C1, N1, C13, Zn and O2 from which O1 deviates by about 0.25 Å. The bromide ligands angle away from this bisecting plane with a Br1-Zn-Br2 angle of 122.86(2)°. The Zn–Br bond distances of 2.3418(4) and 2.3187(4) deviate by more than 0.001 Å and could therefore be distinguished at the 99% confidence level. However, in comparison to the range 2.30 – 2.47 and mean of 2.359 Å for 68 such bonds in the CSD, they both appear to be perfectly normal zinc(II)–bromide bonds. Notably, the longer bond is to Br1 which is involved in hydrogen bonding (see below).

The complex of **1** with zinc(II) chloride, **3**, is isostructural (Figure 2) with that of the bromide **2** and all dimensions are similar except that the Zn-Cl bond lengths are 6.25% shorter than Zn-Br, reflecting the larger covalent radius of Br compared to Cl. In **3**, the Zn–Cl distances to Cl1 at 2.204(2) and to Cl2 at 2.182(2) are also just distinguishable at the 99% confidence level, despite the higher experimental s.u. The longer distance is also to the chloride ligand that hydrogen bonds to the NH of a neighbouring atom in the lattice. The range over 179 structures in the CSD is 2.15 to 2.30 Å with a mean of 2.204 Å, thus these are also entirely normal Zn–Cl bond lengths.

The lattice structures of complexes **2** and **3** consist of infinite hydrogen-bonded chains described by a $C_1^1(6)$ graph set.[28] One set of chains lies parallel to the *ab* plane and approximately perpendicular to the bisector of ∠*ab*, and a second set is related to the first by the *c*-glide operation, so that this chain lies along the bisector direction. The chains strongly resemble those of ligand **1**, but with the insertion of a Zn–Br(Cl) bond between the N–H and O=C groups, resulting in Br(Cl)···O=C hydrogen bonds. The additional spacing allows all the Dipp groups to point in one direction and the ^{t}Bu groups in the opposite, so the chain components are superimposable along the chain direction. THF ligands fill the 'gaps' between Dipp aryl rings.

Table 3. Hydrogen-bonding parameters for the crystal structures of **2** to **4**.

Structure	Donor	H	Acceptor	d(D-H)/Å	d(H-A)/Å	d(D-A)/Å	∠D-H-A/°
1	N1	H1	O1[a]	0.891(16)	1.990(17)	2.814(7)	153.0(13)
ICEXEW [15]	N1	H1	O1[a]	0.880	1.973	2.771(3)	150.3
2	N1	H1	Br1[b]	0.77(2)	2.82(3)	3.501(2)	150(3)
3	N1	H1	Cl1[c]	0.86(3)	2.57(4)	3.352(5)	153(5)
3a	N1	H1	Cl1[d]	0.98(9)	2.50(9)	3.425(4)	157(6)
	C1S	H1S	Cl1	1.00	2.60	3.511(8)	152.0
4	N1	H1	Cl2[e]	0.84(4)	2.49(4)	3.301(3)	163(4)

Symmetry codes: [a] *x*, ½-*y*, ½+*z*; [b] ½+*x*, -½+*y*, *z*; [c] ½+*x*, -½+*y*, *z*; [d] *x*, 1+*y*, *z*; [e] 1½-*x*, -½+*y*, 1½-*z*.

Of some 26 structures containing amide oxygen coordinated to Zn(II) dihalides from a search of the CSD, only two display hydrogen bonding between amide NH and a halogen (YILXIB and YILXOH).[14] These can also be described by $C_1^1(6)$ graph sets like **2** and **3** in space groups $P2_1/c$ and $P\bar{1}$, respectively. A $ZnCl_2$ complex of a bifunctional amide, CSD refcode: EQIGOC, has H-bonding from the coordinated amine NH to the uncoordinated *para* amide oxygen atom, resulting in a zig-zag chain structure linking the L_2ZnCl_2 moieties.[8] Like this example, most known amide complexes of zinc(II) halides have two attached amides, but as tertiary amides lack the NH group and are thereby incapable of hydrogen-bond donation. There are two structures of zwitterionic mono oxygen-bound amides $LZnCl_3$, refcodes: NOGMED and RUJXEA,[12,13] where the ligands L are cationic 3° polycyclic

amides. All other $LZnX_2$ structures in the literature involve bidentate ligands in which an amide donor is combined with another, usually stronger, Lewis acid, such as pyridine nitrogen donors. A review of these literature structures strongly suggests that it is the high steric bulk of **1** due to the combination of the DippN and backbone ^{t}Bu substituents, that is responsible for the mono-amide formulation (and thus retention of coordinated THF).

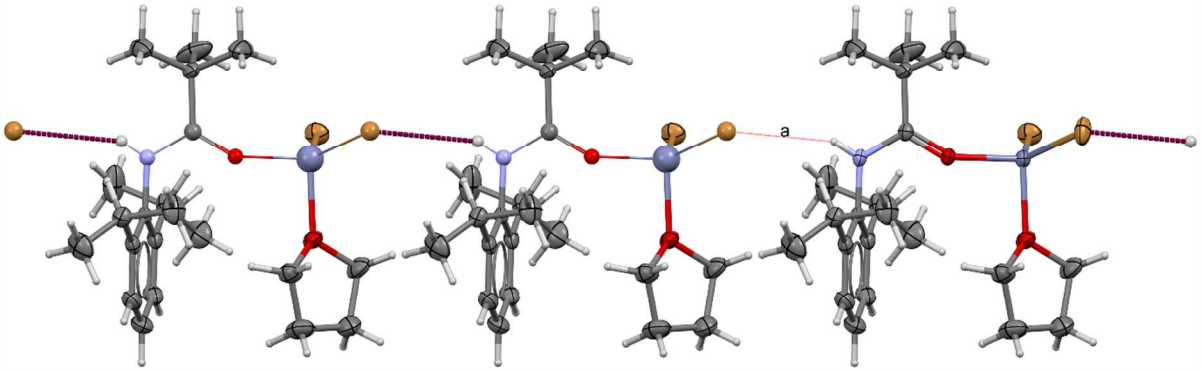

Figure 2. The hydrogen-bonding chain in the crystal lattice of **2** (**3** is isostructural with Cl in place of Br). Grey = C, white = H, red = O, blue = N, dark blue = Zn, bronze = Br. The $C_1^1(6)$ graph set is identified at 'a'.

The lattices in **2** and **3** are densely packed without void spaces, so it is therefore quite surprising to find that **3** also crystallizes in a different polymorph that contains solvent chloroform, i.e. **3a** (Figure 3). This structure, in the non-polar space group $P2_1/c$, also consists of a $C_1^1(6)$ motif with Cl1····O=C hydrogen bonds. In addition, there are terminal non-classical Cl_3C–H····Cl1 hydrogen bonds linking the chain-forming chloride ions to the solvate molecules. Noticeably, the main hydrogen-bonded chain is strikingly similar in the two structures (see Figure S3 in the Supporting Information for a graphical overlap of the two structures.) In **3a**, the chains are strictly parallel to the cell *b* axes and chains are related to each other by the 2_1 axes and inversion symmetry centres. The resultant crystal packing positions all the chloroform solvate molecules in a central slice astride the ½ 0 0 planes. The volume of the lattice in **3a** is 18.5% larger than that of **3** to accommodate the chloroform molecules.

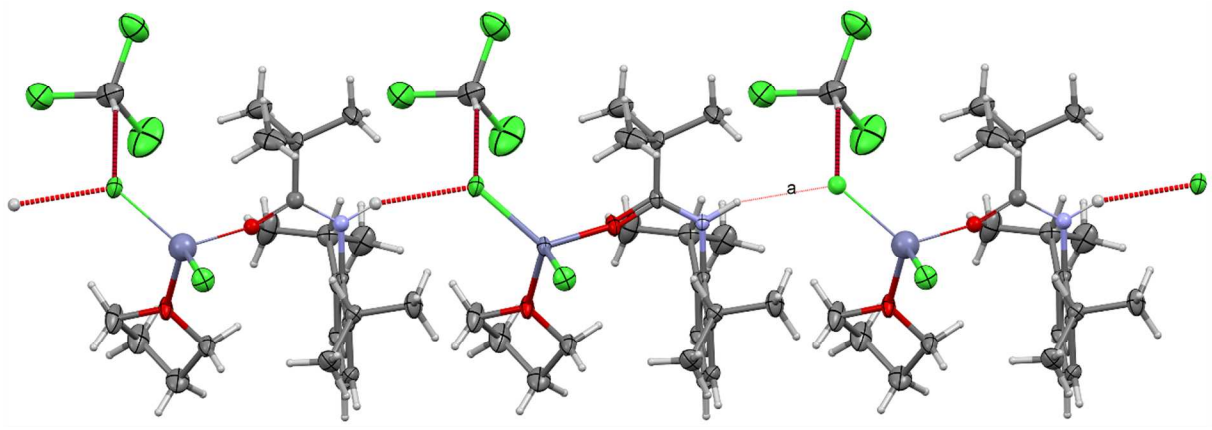

Figure 3. The hydrogen-bonded chain along the crystallographic *b* axis in **3a** showing the additional terminal H-bonds to the $CHCl_3$ solvate molecules. Grey = C, white = H, red = O, blue = N, dark blue = Zn, green = Cl. The $C_1^1(6)$ graph set is identified at 'a'.

In the molecular structure of **3a**, the bond lengths Zn–Cl1 at 2.2236(15) Å and Zn–Cl2 at 2.1860(16) Å are distinguishable at the 99% confidence level just as for the two non-solvated halide complexes, and the longer bond is again that involved in the hydrogen boding to the amide NH hydrogen. The great similarity in structure and bonding of all these complexes of **1** with zinc(II) halides is quite striking.

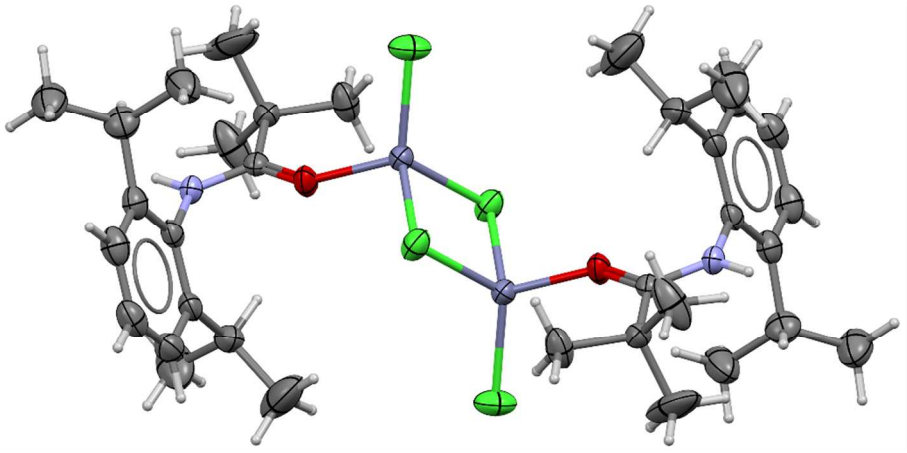

Figure 4. The molecular structure of the centrosymmetric dimer formed by chloro-bridging for the non-solvated amide complex **4**. Grey = C, white = H, red = O, blue = N, dark blue = Zn, green = Cl.

This pattern continues in the rare chloro-bridged dimeric structure **4** (Figure 4), the only mono-amide complex of zinc(II) to possess this stoichiometry. Remarkably, the local geometry at ligand and zinc is similar to that in **2** (see Figure S4 in the Supporting Information). However, it is now Cl2 with the shorter 2.1827(11) Å length that hydrogen bonds to the neighbouring NH hydrogen atom, while bridging Cl1', with Zn–Cl = 2.3250(11) Å, replaces Cl1 in **3** and **3a** and the second bridging Cl1, with Zn–Cl = 2.2996(11) Å, replaces the THF oxygen donor

atom in the non-bridged structures. At the 99% confidence level, all three Zn-Cl distances in **4** are distinguishable. However, in comparison to the eleven comparable L(Cl)Zn-(μ_2Cl)$_2$-Zn(Cl)L structures in the CSD (refcodes: CORRAD,[21] ESOFUP,[22] GORROU,[23] LUZVEI,[24] NABFAZ,[25] ONOMAH,[26] PAFZUU,[27] UYETUO,[28] VALVAH,[29] VULJAN,[30] XONKUI [31]), these sort clearly into longer bridging, mean 2.36(1) Å, and shorter terminal, mean 2.20(1) Å, sets, after removal of single outliers. The effect of bridging on the lengthening of the zinc-chloride bond is larger than that of participation in hydrogen bonding to the amide. Also statistically significant is the zinc(II) to amide oxygen distance of 1.937(2) Å, about 2% shorter than the average over the three non-bridged complexes, indicating that the metal atoms in the Zn_2Cl_4 moiety are better Lewis acids than those in $ZnCl_2$THF. All other intramolecular dimensions other than angles involving chlorides are statistically similar in **4** and the other complexes, as they are to amide **1**.

The lattice structure of **4** has beautiful symmetry. The hydrogen-bonding network (Figure 5) forms layers along the $10\bar{1}$ lattice planes with an interplanar separation of 7.628(1) Å. All the heteroatoms are concentrated at the layer centres. The outer, hydrocarbon, edges of each layer do not interact with neighbouring layers at distances less than the sums of their v. d. Waals' radii. The planes are defined by the midpoints of the Zn-(μ_2Cl)$_2$-Zn moieties, which are through lattice $\bar{1}$ centres. The Zn, O1 and Cl2 atoms are closest to the planes and the Cl2 atoms are approximately perpendicular to them (see Figures S5 and S6 in the Supporting Information). Within these layers, there are $C_1^1(6)$ chains linking the nearest zinc atoms *via* the coordinated amide oxygen over an N–H···Cl hydrogen bond, and $C_1^1(8)$ chains to the farther zinc atom of the μ-Zn_2Cl_2 moieties. $C_2^2(16)$ chains link two μ-Zn_2Cl_2 dimers via amide hydrogen bonds. $R_4^4(28)$ rings describe the smallest molecular "squares" within the layers and these link two μ-Zn_2Cl_2 units at opposite corners with O–Zn–Cl units at the remaining corners (so that the squares have two-fold symmetry consistent with the monoclinic crystal class). Additionally, $R_6^6(44)$ rings extend over two adjacent such "squares".

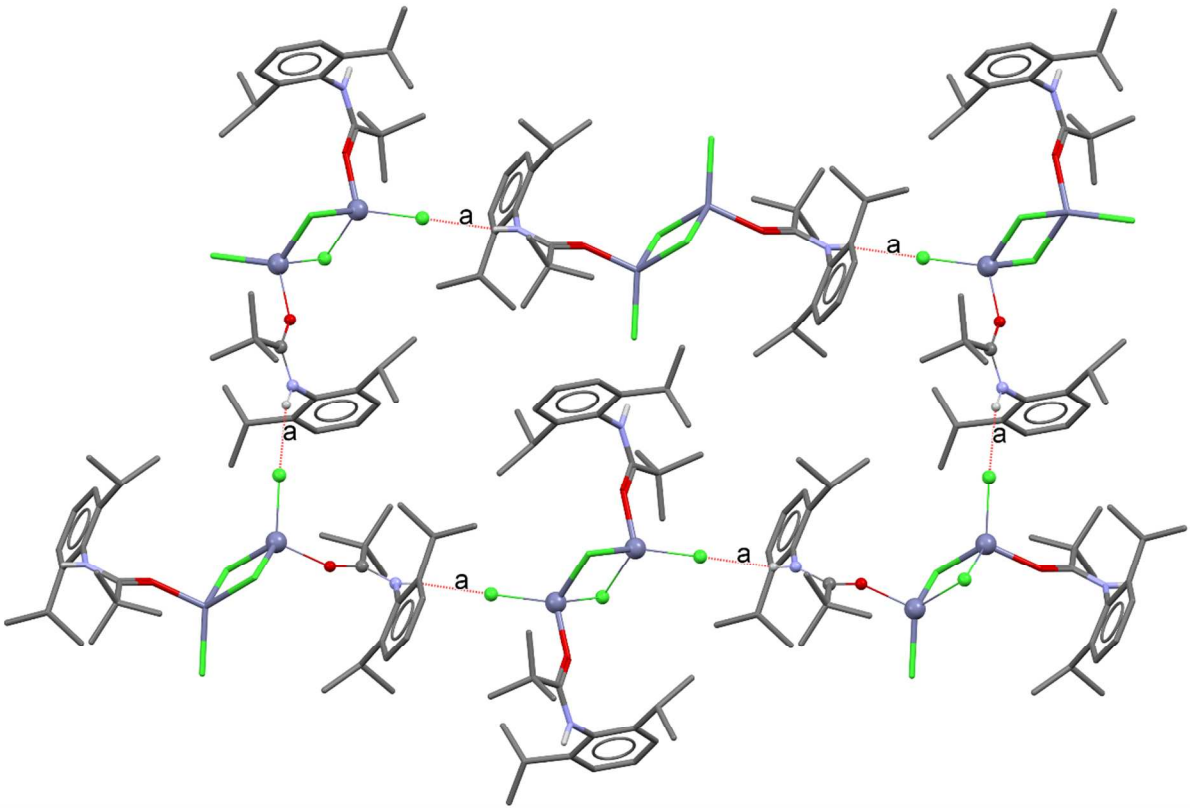

Figure 5. The hydrogen bonding motifs found within layers in the crystal structure of **4** showing the larger $R_6^6(44)$ nets.

The eleven previously reported $[LZnCl_2]_2$ chloro-bridged dimers show surprising diversity in donor ligands L. In CORRAD, L is the ylid Ph_3PCH_2;[29] and in XONKUI the carbon of a conventional NHC.[30] In ESOFUP L is an amidinate-stabilized silylene,[31] whereas in ONOMAH, L is an N-heterocyclic germylene.[32] In GORROU, a terminal rhenium nitride group coordinates to zinc [33] in UYETUO it is the nitrogen from a cyano group coordinated to nickel(II),[34] while in VULJAN the terminal oxide of a Nb(V) complex coordinates almost linearly to zinc.[35] In IJAWUM, L are ethyl groups, affording a rare dianionic diethyltetrachlorodizincate.[36] In LUZVEY,[37] the donor is a phosphine also bearing a pendant 2-anilino group that remains uncoordinated at N, while in PAFZUU the ligand is $^tBu_3P$.[38] In NABFAZ and VALVAH, the donors are phosphinimine N atoms.[39,40] The structure of YOQCUD differs by having five-coordinate zinc atoms, perhaps because the *o*-anisolyl-2-oxozolidine ligand is chelating albeit with a long Zn–O bond of 2.56 Å.[41] Despite this huge diversity in the period, hard/soft donation and element group of these donors, the geometries of the common Zn and Cl components as well as the relative *trans* orientation of L are quite uniform (as already discussed). $^tBu_3P$ forms an especially interesting

comparison with amide **1**. When this phosphine is reacted under anhydrous conditions and in the absence of a Lewis-base solvent, the chloro-bridged dimer PAVZUU forms,[38] but in the presence of THF, monomeric dichlorido(tetrahydrofuran-*κ*O)-(tri-*tert*-butylphosphine-*κ*P)zinc, [(^{t}Bu$_3$P)(THF)ZnCl$_2$], (PAGBAD), is the product.[38] This latter complex bears a strong structural resemblance to that of **3**. Unlike **3** and **4**, these phosphine complexes are quite sensitive to moisture and hydrolyze to ionic salts [HP^{t}Bu$_3$][(H$_2$O)ZnCl$_3$]. This highlights the results of our investigation which indicates that neutral amides are excellent ligands for zinc(II) halides and are better matched as hard bases to zinc halides than the soft-base phosphines. As shown here, bulky secondary amides of the kind that are common precursors to amidates **B** are potent ligands in their own right, whose coordination chemistry is expected to grow in importance with the increased utilization of anionic amidate supporting ligands. Unlike the latter, they demonstrate intriguing and sometimes complex hydrogen-bonded supramolecular architectures.

Supplementary material

Supplementary material is available with the article through the journal Web site at http://nrcresearchpress.com/doi/suppl/xx.yyyy/cjc-2018-zzzz. Structure depositions: archival data has been deposited with the Cambridge Crystallographic Database under CCDC 1562415-1562419. These data can be obtained, free of charge, via http://www.ccdc.cam.ac.uk/products/csd/request/ (or from the Cambridge Crystallographic Data Centre, 12 Union Road, Cambridge CB2 1EZ, UK; Fax: 44-1223-336033 or e-mail: deposit@ccdc.cam.ac.uk).

Acknowledgements

Financial support of this work by the Natural Sciences and Engineering Research Council of Canada is gratefully acknowledged. L.M.A. thanks the University of Lethbridge for a doctoral studentship. The diffractometer was purchased with the help of NSERC-C and the University of Lethbridge. Karen Graham is thanked for assistance with experiments.

References

1. Parkin, G.; *Chem. Rev.* **2004**, *104*, 699. doi:
2. Liang, J.; Lipscomb, W. N. *Biochemistry* **1989**, *28*, 9724. doi
3. Cousins, R. J. *Proc. Nutr. Soc.* **1998**, *57*, 307. doi:
4. Frederickson, C. J.; Koh, J.-Y.; Bush, A. I. *Nat. Rev. Neurosci.* **2005**, *6*, 449. doi:
5. Fraker, P. J.; King, L. E., *Annu. Rev. Nutr.* **2004**, *24*, 277. doi:
6. Pavletich, N. P.; Pabo, C. O. *Science* **1991**, *252*, 809. doi:
7 Schwabe, J. W. R; Rhodes, D. *Trends Biochem. Sci.* **1991**, *16*, 291. doi:
8. Sultana, K.; Zaib, S.; Khan, N. u. H.; Khan, I.; Shahid, K.; Simpson, Jim; Iqbal, J. *New J. Chem.* **2016**, *40*, 7084. doi:10.1039/C5NJ03531G.
9. Bekaert, A.; Lemoine, P.; Brion, J.D.; Viossat, B. *Acta Crystallogr., Sect. E: Struct. Rep. Online* **2003**, *59*, m574. doi:10.1107/S1600536803014570.
10. Gao, J.; Martell, A. E.; Reibenspies, J. *Helv. Chim. Acta* **2003**, *86*, 196. doi:10.1002/hlca.200390011.
11. Savinkina, E. V.; Buravlev, E. A.; Zamilatskov, I. A.; Albov, D. V. *Acta Crystallogr., Sect. E: Struct. Rep. Online* **2007**, *63*, M1094. doi:10.1107/S1600536807011944.
12. Przybyl, A.; Kubicki, M.; Jastrzab, R. *J. Inorg. Biochem.* **2014**, *138*, 47. doi:10.1016/j.jinorgbio.2014.04.015.
13. Jin, Z. M.; Ma, L. L.; Wei, W. X.; Li, Y. Q. *Zh. Strukt. Khim.* **2009**, *50*, 197. doi:
14. Chaudhuri, U.P.; Whiteaker, L. R.; Mondal, A.; Klein, E. L.; Powell, D. R.; Houser, R. P. *Inorg. Chim. Acta* **2007**, *360*, 3610. doi:10.1016/j.ica.2007.05.003
15. Beattie, D. D.; Bowes, E. G.; Drover, M. W.; Love, J. A.; Schafer, L. L. *Angew. Chem. Int. Ed.* **2016**, *55*, 13290. doi:
16. Eisenberger, P.; Ayinla, R. O.; Lauzon, J-M. P.; Schafer, L. L. *Angew. Chem. Int. Ed*. **2009**, *48*, 8361. doi:
17. Drover, M. W.; Schafer, L. L.; Love, J. A. *Organometallics* **2015**, *34*, 1783. doi:10.1021/om501209c.
18. Saalfrank, R. W.; Reimann, U.; Göritz, M.; Hampel, F.; Scheurer, A.; Heinemann, F. W.; Büschel, M.; Daub, J.; Schünemann, V.; Trautwein, A. X. *Chem. Eur. J.* **2002**, *8*, 3614. doi:
19 Armarego, W. L. F.; Perrin, D. D. *Purification of Laboratory Chemicals*, 4th Ed. Oxford: Butterworth & Heinemann, p. 452.
20 Boudjouk, P.; So, J. H.; Ackermann, M. N.; Hawley, S. E.; Turk, B. E., *Inorganic Syntheses* **1992**, 29, 108-111.
21 Bruker, APEX2, SAINT-Plus and SADABS. Bruker AXS Inc., Madison, Wisconsin, USA., 2008.
22 Sheldrick, G. M. *Acta Cryst*. **2008**, A*64*, 112. doi:
23 Sheldrick, G. M. *Acta Cryst.* **2015**, A*71*, 3. doi:10.1107/S2053273314026370.
24 Sheldrick, G. M. *Acta Cryst.* **2015**, C*71*, 3. doi:10.1107/S2053229614026540.
25 Dolomanov, O. V.; Bourhis, L. J.; Gildea, R. J.; Howard, J. A. K.; Puschmann, H. *J. Appl. Cryst.* **2009**, *42*, 339. doi:10.1107/S0021889808042726.
26 Macrae, C. F.; Edgington, P. R.; McCabe, P.; Pidcock, E.; Shields, G. P.; Taylor, R.; Towler, M.; van de Streek, J. *J. Appl. Cryst.* **2006**, *39*, 453. doi:

27 Allen, F. H. *Acta Cryst*. **2002**, B*58*, 380. doi:
28 Etter, M. C.; MacDonald, J. C.; Bernstein, J. *Acta Cryst*. **1990**, B*46*, 256. doi:
29 Pattacini, R.; Jie, S.; Braunstein, P. *Chem. Commun.* **2009**, 890. doi:10.1039/b817728g.
30 Fliedel, C.; Mameri, S.; Dagorne, S.; Aviles, T. *Appl. Organomet. Chem.* **2014**, *28*, 504. doi:10.1002/aoc.3154.
31 Schafer, S.; Koppe, R.; Roesky, P. W. *Chem.-Eur.J.* **2016**, *22*, 7127. doi:10.1002/chem.201505001.

32 Sinhababu, S.; Yadav, D.; Karwasara, S.; Sharma, M. K.; Mukherjee, G.; Rajaraman, G.; Nagendran, S. *Angew. Chem. Int. Ed.* **2016**, *55*, 7742. doi:10.1002/anie.201601445

33 Hagenbach, A.; Strahle, J. *Z. Anorg. Allg. Chem.* **1999**, *625*, 1181. doi:10.1002/(SICI)1521-3749(199907)625:73.0.CO;2-Z.

34 Tauchert, M. E.; Warth, D. C. M.; Braun, S. M.; Gruber, I.; Ziesak, A.; Rominger, F.; Hofmann, P. *Organometallics* **2011**, *30*, 2790. doi:10.1021/om200164f.

35 Fu, P-F; Khan, M. A.; Nicholas, K. M. *Organometallics* **1992**, *11*, 2607. doi:10.1021/om00043a051.

36 MacIntosh, I. S.; Sherren, C. N.; Robertson, K. N.; Masuda, J. D.; Pye, C. C.; Clyburne, J. A. C. *Organometallics* **2010**, *29*, 2063. doi:

37 Liang, L-C.; Lee, W-Y.; Tsai, T-L.; Hsu, Y-L.; Lee, T-Y. *Dalton Trans.* **2010**, *39*, 8748. doi:10.1039/c0dt00327a.

38 Finke, A. D.; Gray, D. L.; Moore, J. S. *Acta Crystallogr., Sect. E: Cryst. Commun.* **2016**, *72*, 35. doi:10.1107/S2056989015023373.

39 Valerio-Cárdenas, C.; Hernández, M-A.M.; Grévy, J-M. *Dalton Trans.* **2010**, *39*, 6441. doi:10.1039/b925580j.

40 Wheaton, C. A.; Ireland, B. J.; Hayes, P. G. *Z. Anorg. Allg. Chem.* **2011**, *637*, 2111. doi:10.1002/zaac.201100355.

41 Gossage, R. A.; Yadav, P. N.; MacInnis, T. D.; Quail, J. W.; Decken, A. *Can. J. Chem.* **2009**, 87, 0368.

Hydrogen-bonded Networks in Oxygen-coordinated Monoamide Complexes of Zinc(II)

Leila Mokhtabad Amrei and René T. Boeré*

Department of Chemistry and Biochemistry *and* the Canadian Centre for Research in Advanced Fluorine Technologies, University of Lethbridge, 4401 University Dr. W, Lethbridge, AB, Canada, T1K 3M4.

Supporting Information

CONTENTS PAGE

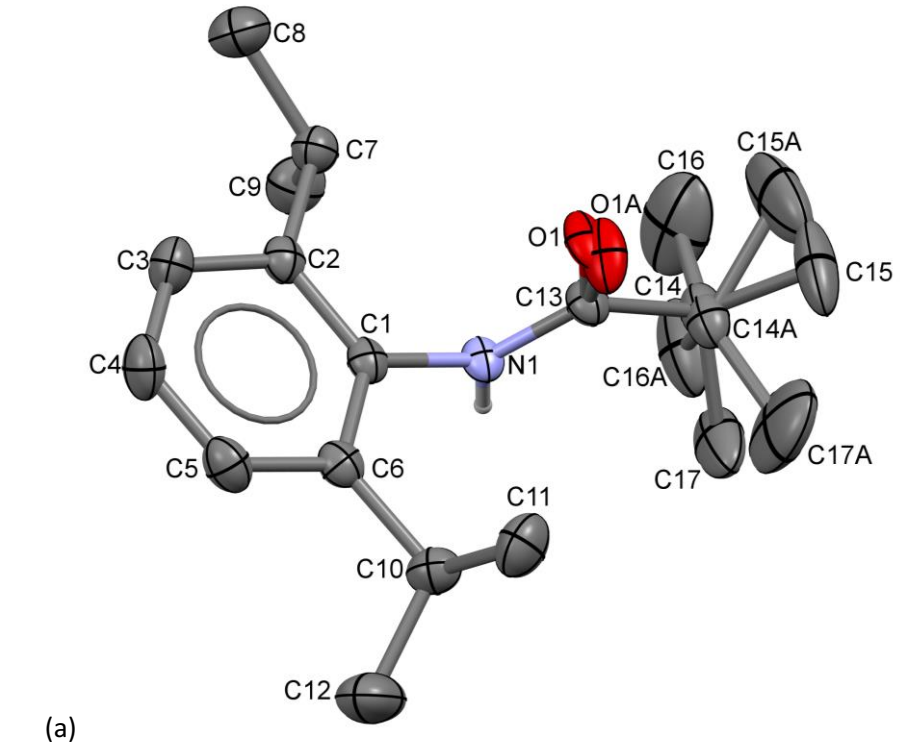

(a)

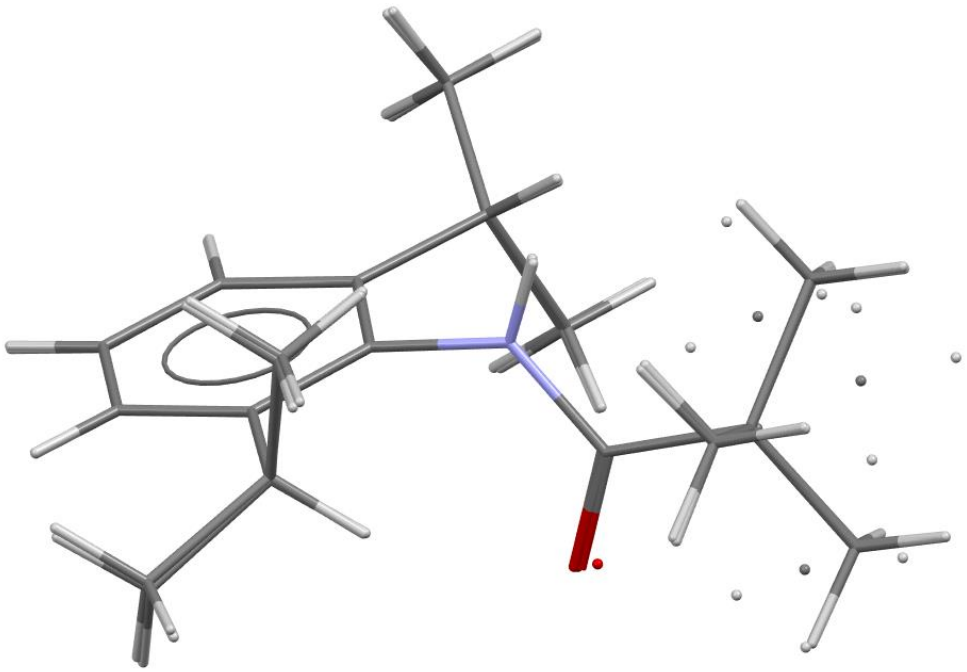

(b)

Figure S1. (a) Molecular structure of **1** showing the atom numbering scheme and the disorder model. (b) Overlay of the molecular structures of **1** and ICEXEW from the respective crystal structures. Deviations occur due to the ^{t}Bu group disorder in **1** as well as minor positional differences for the ^{i}Pr groups.

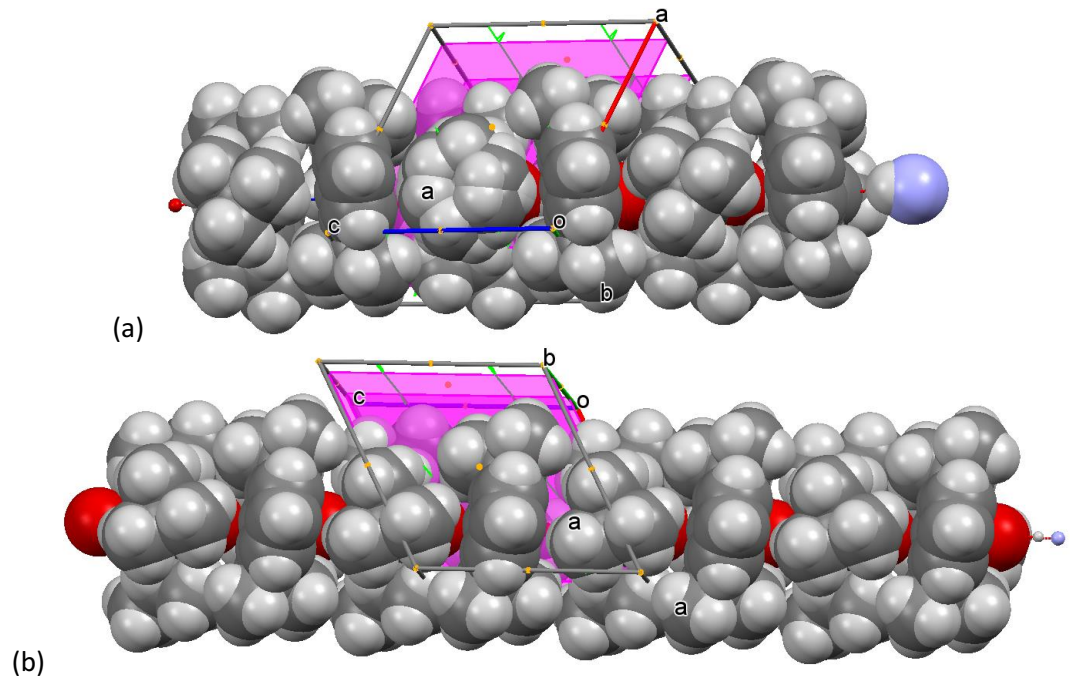

Figure S2. (a) Disordered and (b) ordered arrangements of the ^{t}Bu groups in the solid-state lattice of **1**.

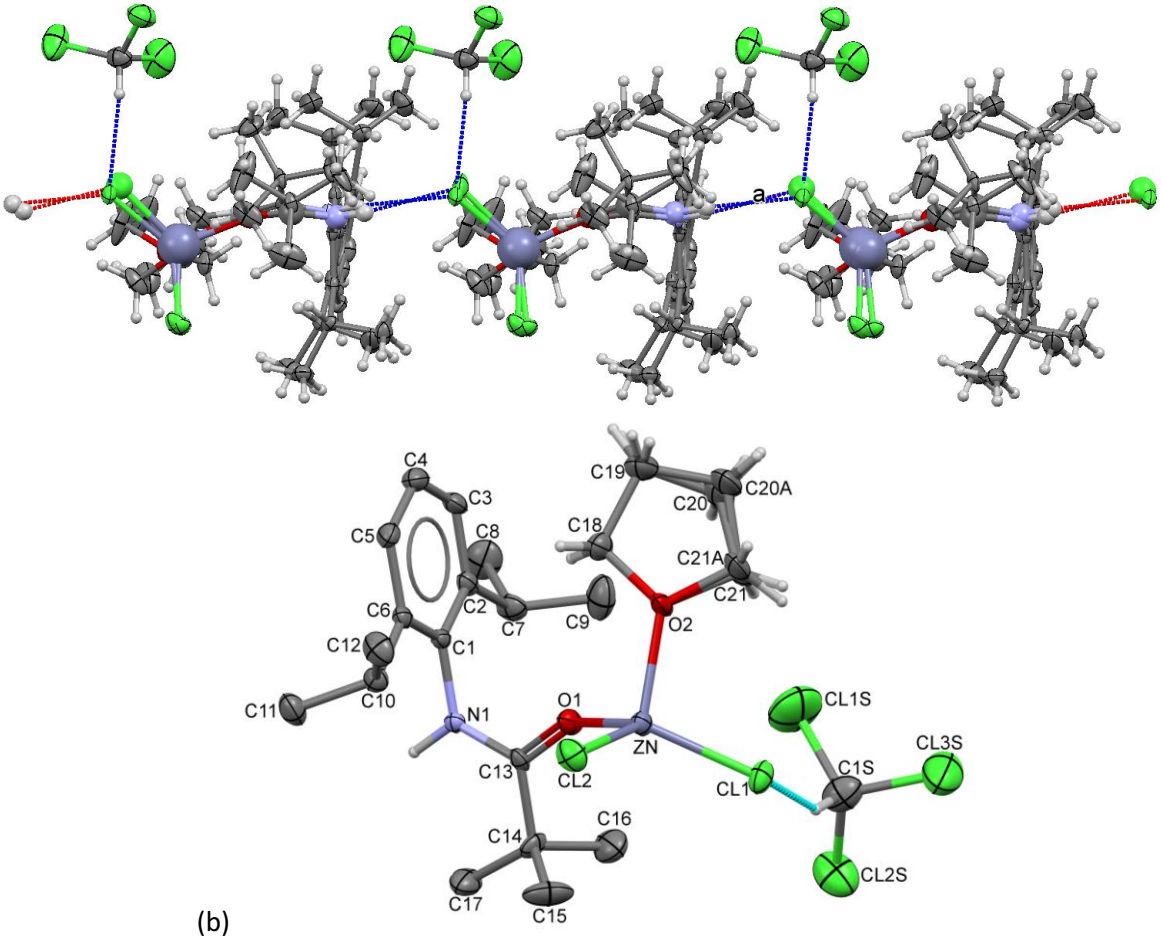

Figure S3. (a) Overlap map of the structures of the hydrogen-bonded chains in the structures of **3** and **3a**. (b) Atom numbering scheme for **3b** and depiction of the THF disorder model.

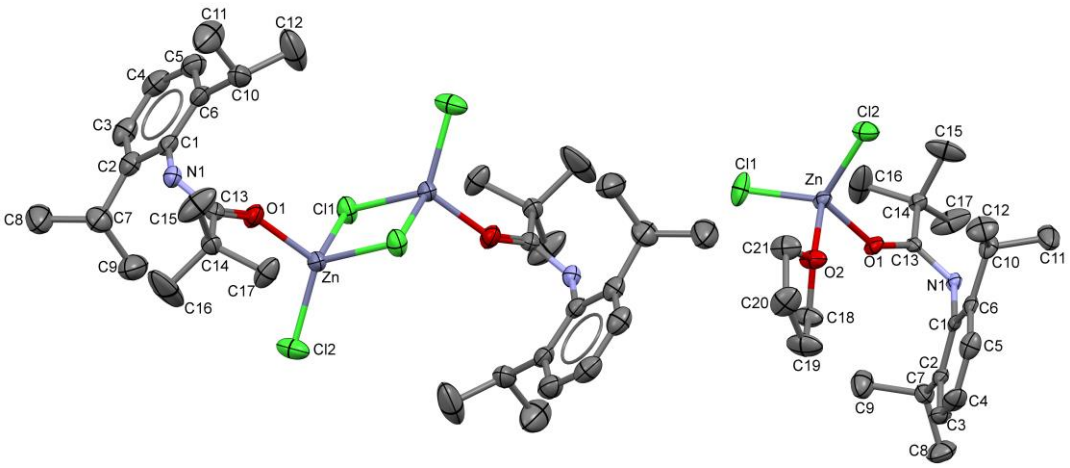

Figure S4. Side-by-side comparison of the local structures of (left) **4** and (right) **3**, showing the similarities in geometry. The unique atom numbering schemes for the two structures (and also for **2** where Br replaces Cl) are also provided.

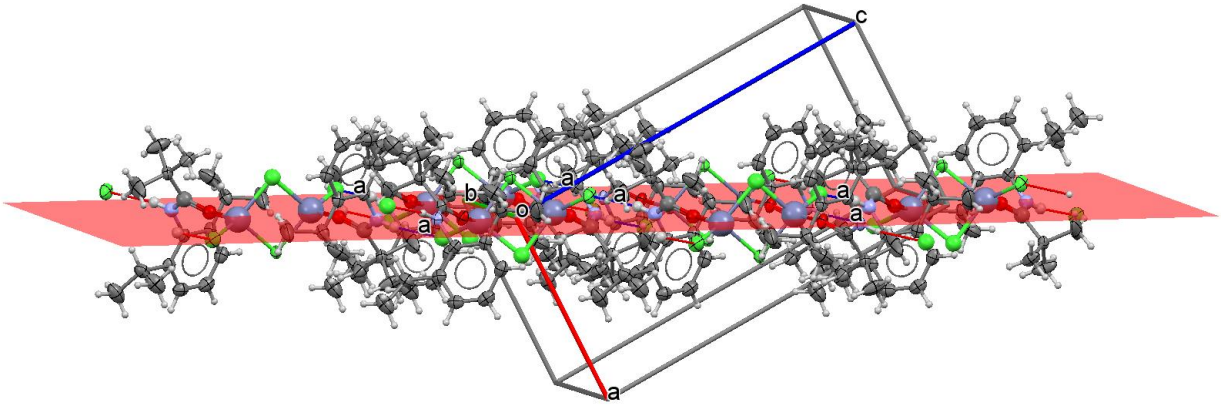

Figure S5. The hydrogen-bonded layers in the structure of **4** along the $\bar{1}01$ lattice plane and thereby parallel to the *b* axis.

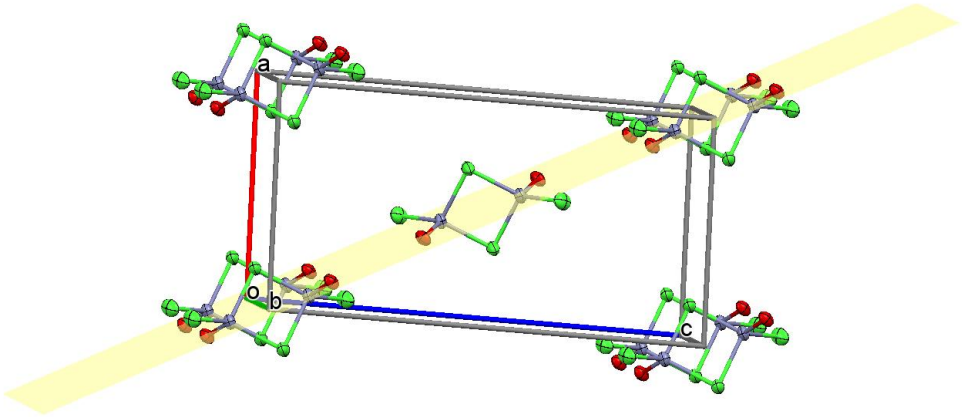

Figure S6. Detail showing the location of the $\bar{1}01$ lattice plane in the unit-cell of **4**. The Zn and O atoms are located closest to the planes, followed by Cl2. Cl1 bridging chlorides are perpendicular to this plane.